Energy Equip. Sys./ Vol. 11/No. 1/March 2023/ 55-68

ENERGY EQUIPSYS

Energy Equipment and Systems

http://energyequipsys.ut.ac.ir

www.energyequipsys.com

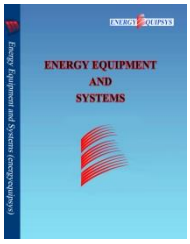

Fabrication and assessment of a parabolic dish concentrator using a water heater cylindrical receiver

Authors

Ali Reshad[a]

Mehrdad Boroushaki [a]*

[a] Department of Energy Engineering, Sharif University of Technology, Tehran, Iran

ABSTRACT

This study presents a novel approach to fabricating a low-cost solar parabolic dish concentrator with one-meter-long glass/silver mirrors on the reflecting surface. The concentrator's parabola curve is made of four layers of fiberglass needle felt and polyester resin. The parabolic dish surface is mirrored vertically with 2 mm thickness glass/silver mirrors with a width of 5 cm and a length of one meter attached with silicone glue. The system is assembled and tested at the Sharif University of Technology in Tehran, Iran. Energy and exergy efficiencies are calculated using cylindrical water heater receiver data. These data are used to calculate the receiver's absorbed energy and losses. Test results show that the major energy loss is due to convection. The average energy efficiency and the maximum exergy efficiency of the concentrator are 57% and 67%, respectively. The maximum power absorbed by the water is 1656.8 W at midday, and the maximum temperature observed on the receiver is 540°C. Finally, a discussion is held to propose ideas to improve the fabrication process of the designed parabolic dish concentrator. This type of fabrication is suitable for regular thermal applications. However, several deficiencies are detected, and a few solutions are suggested. Mirror edges and flexibility are two of the parabolic dish's major defects.

Article history:

Received : 7 September 2022

Accepted : 2 February 2023

Keywords: Solar Energy; Parabolic Dish Fabrication; Solar Concentrator; Receiver; Efficiency

1. Introduction

Overpopulation and industrial evolution have brought a tremendous increase in energy demand, and all countries, especially developing countries, are forced to search for energy sources [1]. Since energy and water supply have become the most critical resources for sustainable development, they are now among the most significant research topics [2]. For decades, coal, oil, and natural gas have been considered the most accessible resources for energy needs [3]. Nevertheless, their limited supply and pollution effects have become the primary constraint on their ability to be the Earth's steady sources [4]. These adverse effects have forced humans to utilize sustainable energy resources instead of fossil fuels, inspiring steadily growing attention to renewable energies [5]. Among the various types of renewable energy resources, solar energy may be the most excellent alternative for the future due to its abundance, inexhaustible supply, and ecological benefits [6]. Solar systems utilize

* Corresponding author: Mehrdad Boroushaki
Department of Energy Engineering, Sharif University of Technology, Tehran, Iran
Email: boroushaki@sharif.edu

solar collectors to collect, store, and apply solar radiation for the benefit of domestic, commercial, and industrial uses [7].

Various applications for solar energy collectors are available, including power generation, water heating and desalination, building cooling and heating, food refrigeration, cooking, crop drying, and heat generation for industries [8]. Solar collectors can be classified as stationary or concentrating [9]. Concentrating solar collectors generally have concave reflecting surfaces to intercept and focus the sun's beam radiation to a smaller receiving area, thereby increasing radiation flux, while stationary collectors have the same area for intercepting and absorbing solar radiation [10]. Solar collectors are distinguished by their motion in three types; stationary, single-axis tracking, and two-axis tracking. Parabolic Dish (PD) concentrators and heliostat field collectors are the two types of two-axis tracking collectors with the highest concentration ratio and temperature range [11]. Two-axis tracking of a collector makes it the more efficient system because it is always pointed toward the sun [12]. Moreover, the PD concentrator has a concentration ratio of 600 to 2000 and is more efficient in thermal energy absorption systems. The system can reach temperatures above 1500 °C [13]. This system can be improved in many ways, including optimizing the collector's performance. Therefore, this topic is an essential topic for researchers [14].

Several studies have been published about the performance assessment of PD concentrators, which offer perspectives to optimize this equipment as a system. Yan et al. [15] proposed two mirror rearranging strategies and their optimization technique by integrating a novel ray tracing method with a genetic algorithm. This optimization aimed to ensure uniform flux distribution on the absorber surface inside the cavity receiver of the parabolic dish concentrator. Hijazi et al. [16] designed a low-cost solar PD with diameters of 5, 10, and 20 m and a focal point-to-aperture diameter ratio of 0.3. Their study focused on selecting the appropriate dimensions of the reflecting surfaces to be cut from the available sheets on the market. This way, the dish's weight, and cost were minimized while providing the least amount of deflection and stress. In another study, Affandi et al. [17] employed Matlab Simulink to design a PD concentrator with a concentrated power of one kW in Malaysia. The paper elaborated on the methodology used to develop the concentrator and outlined the parameters needed to improve its efficiency. They suggested using aluminum as a reflective material for the concentrator.

Li et al. [18] investigated a PD concentrator mirror formed from several thin flat metal petals with highly reflective surfaces through numerical and experimental practices. They offered an easier way to fabricate and package flat mirrors and provided a convenient shipping process to field sites and assembly. Aljabair et al. [19] introduced a method to design and fabricate a solar thermal collector using a PD and a cavity receiver, considering simple materials at low cost. In the PD fabrication process, nickel sheet metal was used as the sunray reflector surface material, which can withstand prolonged exposure to sunlight and temperatures as high as 80 °C without losing any of its properties. Their results were limited to water temperature and pressure variation in the cavity receiver. Masum Ahmed et al. [20] designed and fabricated a parabolic solar cooker using different reflective materials such as stainless steel, aluminum foil, and Mylar tape. Mylar tape had more successful results than the other two materials. Their results were confined to evaluating the temperature of the receiver. Velimir et al. [21] investigated solar dish collector parameters with a spiral-coil absorber, including inlet temperature, flow rate, absorber emittance, optical efficiency, wind velocity, and ambient temperature. The dish reflector they examined and assessed was constructed of 11 curvilinear trapezoidal reflective petals made of polymethyl methacrylate coated with silver. In another study, a simple laboratory-scale parabolic concentrator was designed, built, and tested by Rafeeua et al. [22]. Three dish concentrators with various parameters were tested in this work. Two dishes were made from acrylonitrile butadiene styrene and another one from stainless steel. They evaluated the efficiency and cost of these concentrators.

Madadi Avargani et al. [23] carried out an exergy and energy analysis on a solar PD col-

lector. A parametric study based on the developed objective function showed that exergy efficiency greater than 20% is attainable. Their PD was fabricated using square mirrors. Savangvong et al. [24] designed, analyzed, fabricated, and tested three economical PD collectors with an aperture diameter of one meter. They used different reflector materials: an emergency blanket, a PET mirror, and a square mirror. Their results showed that the maximum temperature of the dish with an emergency blanket, polyethylene terephthalate mirror, and glass/silver mirror was 817 °C, 724 °C, and 874 °C, respectively. They also revealed that their PDs were capable of concentrating heat at 389 W, 361 W, and 420 W, respectively. Sahu et al. [25] presented a novel approach to designing and developing a low-cost solar parabolic dish concentrator with a 12.6 m^2 aperture area. Their PD concentrator consists of 12 petals, where each petal is supported by a truss structure. They used silver-backed square mirrors as reflective surfaces. Their results were primarily based on cost analyses rather than technical evaluations. Finally, Gholamalizadeh and Chung [26] carried out energy and exergy analyses for a pilot parabolic solar dish-Stirling system. Their PD consisted of square 0.08 m × 0.08 m glass/silver mirror panels with a thickness of 2 mm. A comparison was also made between their results and those of EuroDish.

Based on the above-mentioned literature, the solar PD concentrator is an interesting and challenging research subject. There was a lack of discussion of fabrication methods and ways to improve this process in most of the articles. This study presents a novel low-cost method for fabricating PD parabola shapes. In addition, unlike most of the articles that used square-shaped mirrors, this paper utilizes one-meter-long low-cost glass/silver mirrors. For assessing the fabricated PD, a cylindrical receiver was heated with this concentrator, and water was used as the heat transfer fluid. The following sections describe the design and fabrication process in detail. Then the PD's performance is evaluated by analyzing the receiver's maximum temperature versus solar radiation intensity, energy efficiency, and exergy efficiency. Finally, a discussion is held to investigate possible fabrication flaws and propose some ideas for improving the concentrator.

2. Materials and Methods

Experimental research in this paper builds and tests a PD concentrator with a cylindrical receiver. A schematic view of the experimental setup is shown in Fig.1. In order to evaluate the concentrator's performance, water is used as a heating fluid. A hydraulic pump transfers water into the receiver cylinder, and it is then cooled by an air-cooled heat exchanger. A container is placed between the heat exchanger and the pump to stabilize the water flow. The loop is completed by pumping water to the receiver. An electric cylinder and a motor coupled with a gearbox are utilized to track the sun during the day. All the system's parts are described in detail in the following sections.

2.1. Parabolic Dish Concentrator

Figure 2 shows the general aspect of a parabolic curve. The rim angle is the angle between the axis and a line from the focal point to the physical edge of the concentrator. Sunbeams are concentrated on the receiver at the focal point.

The following equation shows the parabolic equation assuming that the vertex of the parabolic curve is at point (0,0):

$$y^2 = 4f_d x, \tag{1}$$

where f_d is the focal length of a parabola. Concentrators with a larger rim angle have steeper slopes. This angle can be calculated with the following equations by knowing the focal length and diameter of the dish [23]:

$$A_c = 4\pi f_d^2 \cdot \frac{\sin^2(\Psi_{rim})}{(1+\cos\Psi_{rim})^2}, \tag{2}$$

$$\Psi_{rim} = \tan^{-1}\left(\frac{\frac{f_d}{d}}{2\left(\frac{f_d}{d}\right)^2 - \frac{1}{8}}\right), \tag{3}$$

where Ψ_{rim} is the rim angle and d is the aperture diameter.

A higher concentration ratio reduces the diameter of the focused part on the receiver, which results in heat loss reduction. The highest concentration ratio theoretically occurs when the rim angle is 45˚. The focal length to aperture diameter ($\frac{f_d}{d}$) for a rim angle of 45˚ is equal to 0.6 [27]. Based on the literature review, an aperture diameter of 2 m to 3 m is suitable for experimental purposes. This study considers a 2 m diameter PD with a rim angle of 45˚, where the focal length equals 1.2 m.

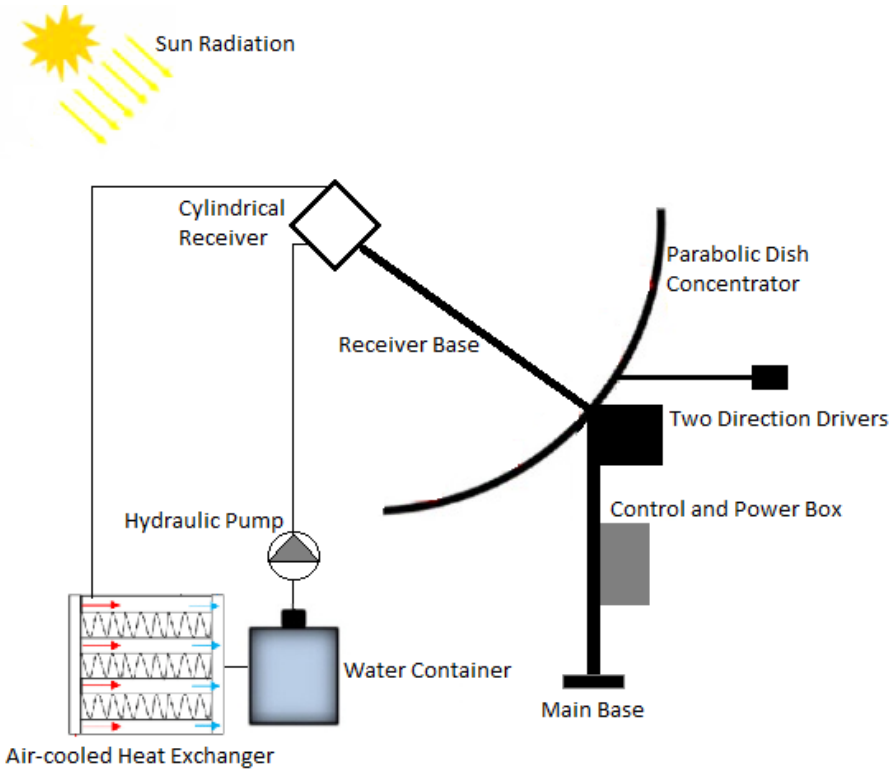

Fig. 1. Schematic View of the Designed Solar Water Heater System

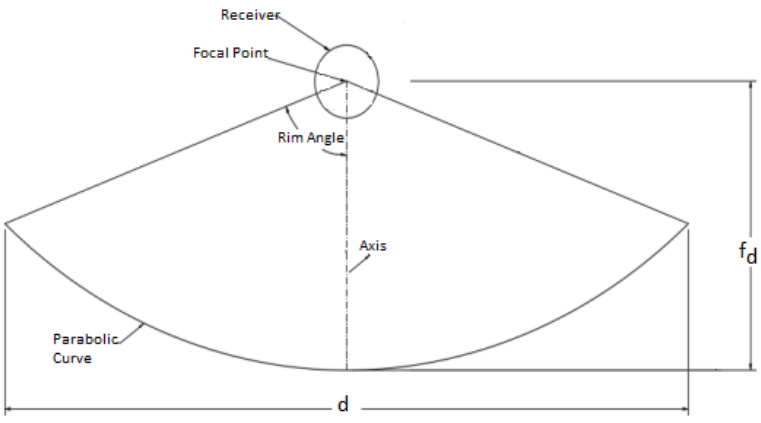

Fig. 2. General Aspect of a Parabolic Curve

2.1.1. Parabolic Dish Fabrication

Figure 3 shows the general steps in the fabrication of the PD. At first, a profile of the parabolic curve is designed with a thickness of 4 mm and a width of 7 cm of Plexiglass. This profile is prepared on a CNC machine and used for making the mold. Then, a metal base is installed on the ground, and a truss-like piece that can rotate around the base axis is installed. The curved dish profile blade is mounted precisely on the base guide, and a gypsum mold is prepared by rotating the blade around the axis to form the shape of the dish (Fig.3-a). After the mold is formed, wax is rubbed on the mold surface to separate the dish easily. Finally, layering is done using fiberglass needle felt and polyester resin (Fig.3-b). The number of resin layers is set to four. When the dish is dried and cleaned (Fig.3-c), the dish's surface is mirrored using silicone glue and 2 mm glass/silver mirrors with a width of 5 cm and a length of one meter (Fig.3-d).

2.1.2. Main Base and Drivers

Figure 4 shows the assembly of the main base and drivers. In this design, the main base and the drivers are located behind the dish to minimize shade and utilize all the dish surfaces to reflect the sunbeams (Fig.4-b). A solar tracker with the ability to adjust the dish azimuth and elevation angles is needed (Fig.4-a). This tracking is done manually with a joystick.

For the azimuth angle, two worm gearboxes are used to rotate the dish, which provides a total ratio of 1400:1 (Fig.4-c). The gearboxes are driven by a 100 W DC electric motor, which lets the dish rotate 360˚ per minute.

An electric screw cylinder with a pitch of 4 mm and a stroke of 60 cm is used for the elevation angle. A worm gearbox with a ratio of 30:1 and a DC electric motor with a power of 100 W is required (Fig.4-d).

Fig. 3. PD Concentrator Fabrication Steps: (a) Gypsum Mold; (b) Layering With Needle Felt and Polyester Resin; (c) Dried Product; (d) Mirrored Dish

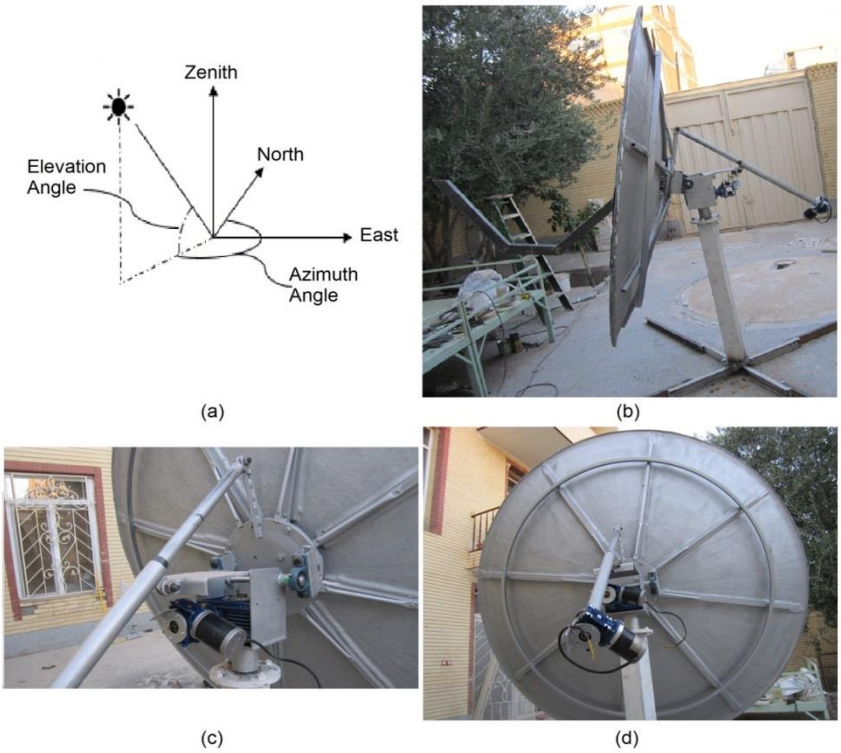

Fig. 4. Main Base and Drivers: (a) Azimuth and Elevation Angle; (b) Assembly; (c) Azimuth Angle Adjustment Mechanism; (d) Elevation Angle Adjustment Mechanism

2.2. Receiver Loop

Figure 5 shows the main parts of the receiver loop: a cylindrical receiver, air-cooled heat exchanger, water container, hydraulic pump, and hose. The receiver housing is made with 0.5 mm thickness stainless steel 316 sheets with a diameter of 20 cm and a height of 20 cm (Fig.5-a). The total mass of the receiver is 752 grams. One port at the bottom for the water inlet and another on the opposite side up for the water outlet are installed. These ports are ¼" G unions welded to the receiver, and the threaded hose is also ¼". The air-cooled heat exchanger is selected from the available Kia Pride automobile aluminum radiator (Fig.5-b). This cooler has approximately 40 kW heat dissipation capacity and is used without a fan motor. A four-liter water container is located in the loop to stabilize the cooling water flow. Finally, a DC motor pump with a flow rate of 0.95 lit/min is used to conduct the water into the cylindrical receiver (Fig.5-b). The water flow rate is selected at a low level because water should have time to absorb concentrated heat. Figure 6 shows the final setup of the receiver part. The radiated sunlight has completely illuminated the hot surface of the receiver. Therefore, the concentrated area on the receiver is considered equivalent to a 20 cm diameter.

2.3. Instruments

For measuring different parameters, precise instruments are used. Table 1 summarizes the parameters and instruments specifications and Fig.7 shows the instruments. The pump's flow rate is determined by a 1.5-liter container and a timer at the outlet of the cylindrical receiver at operational height. A Testo laser thermometer is used to measure temperature changes in the receiver (Fig.7-c). For calibration of the thermometer, the surface emissivity coefficient should be determined. As a result, the receiver surface is coated with high-temperature resistant Ambro-Sol spray matte black. This way, the emissivity coefficient becomes 0.98; a type K thermocouple is also used to validate this value.

Fig. 5. Receiver Loop Parts: (a) Cylindrical Receiver; (b) Air-cooled Heat Exchanger and DC Motor Pump

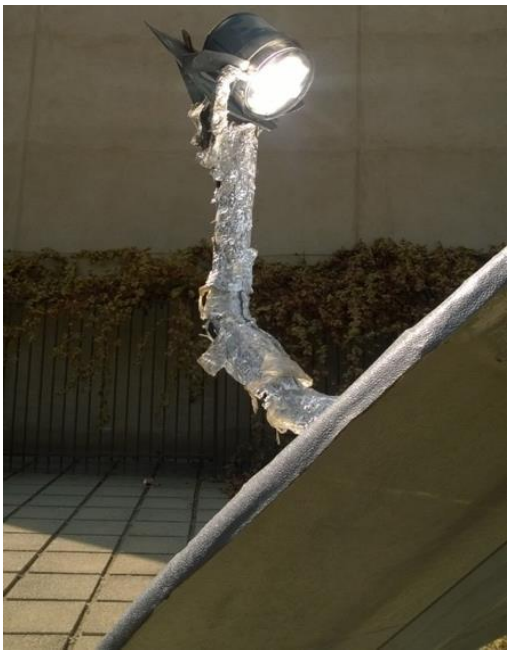

Fig. 6. The Final Setup of the Receiver Part

Table 1. Instruments Summary

Instrument	Parameter	Accuracy	Range
Type K Thermocouple	Water Inlet and outlet Temperatures	± 1.5 K between -40 and 375 °C	-270 to 1260 ℃
Sunny Sensorbox	Sun Irradiation Intensity	± 8 %	0-1500 W/m^2
Sunny Sensorbox (PT100)	Ambient Temperature	± 0.5 ℃	-20 to 110 ℃
Sunny Sensorbox (Spoon Anemometer)	Wind Speed	± 0.5 %	0.8 to 40 m/s (max. 60 m/s short term)
Testo 881	Cylindrical Receiver Surface Temperature	± 2 ℃	-20 to 350 ℃ 350 to 550 ℃

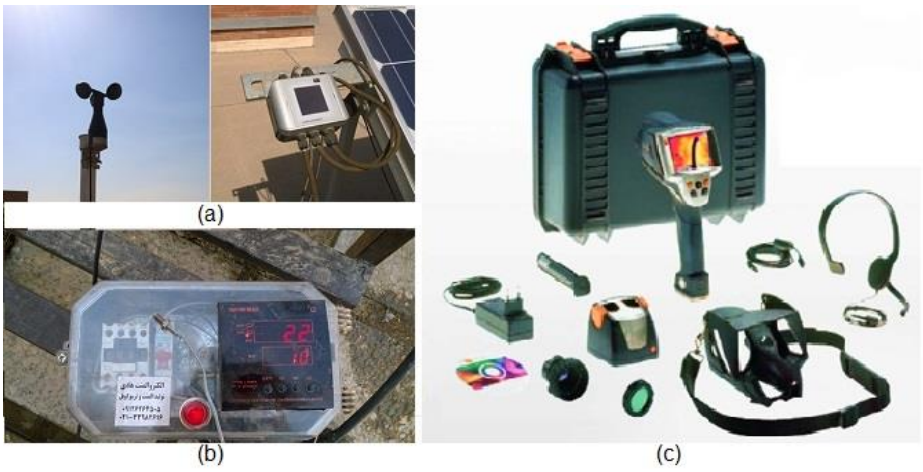

Fig. 7. Instruments Used in This Study: (a) Sunny Sensorbox; (b) Type K Thermocouple; (c) Testo 881

2.4. Parabolic Dish Concentrator Performance

The concentrated heat in the receiver includes the heat absorbed by the water inside the receiver and the heat losses. There are several sources of heat loss, including radiation, convection, and conduction. As a result, the total PD energy efficiency (η_{en}) can be calculated by

$$\eta_{en}=\frac{Q_{rec}}{Q_a}=\frac{Q_w+Q_{rad\_r}+Q_{rad\_p}+Q_{conv}+Q_{cond}}{Q_a}, \quad (4)$$

where Q_{rec} is the total incident heat on the receiver (watts), Q_w is the absorbed heat by the water (watts), Q_{rad_r} is the receiver's hot surface radiation heat loss (watts), Q_{rad_p} is the receiver's peripheral surface radiation heat loss, Q_{conv} is the heat loss by the wind flow (watts), Q_{cond} is the conduction heat loss (watts), and Q_a is the incident radiation heat on the PD (watts).

The incident radiation heat on PD is obtained by

$$Q_a=I_{sun}*A_a, \quad (5)$$

where I_{sun} is the intensity of solar radiation (watts per square meter), and A_a is the aperture area of the dish (m^2) [28].

The heat absorbed by water is calculated from

$$Q_w=\dot{m}c\Delta T_w \quad (6)$$

where $\dot{m}$ is the flow rate of the water (kg/sec), c is the specific heat capacity of water, which is 4182 J/kg°C, and ΔT_w is the difference between outlet and inlet temperatures of the water (K) in the receiver.

The radiation heat losses can be calculated from

$$Q_{rad-r}=\epsilon\sigma({T_{rec-r}}^4-{T_{amb}}^4)A_r \quad (7)$$

$$Q_{rad-p}=\epsilon\sigma({T_{rec-p}}^4-{T_{amb}}^4)A_p \quad (8)$$

where ϵ is the receiver's surface diffusion coefficient (between 0 and 1), σ is the Boltzmann constant (5.6703×10^{-8} w/m^{2}K^4), T_{rec_r} is the receiver's hot surface temperature (K), T_{rec_p} is the receiver's peripheral surface temperature (K), T_{amb} is the ambient temperature (K), A_r is the receiver's hot surface area (m^2), and A_p is the receiver's peripheral surface area (m^2) (Fig.8).

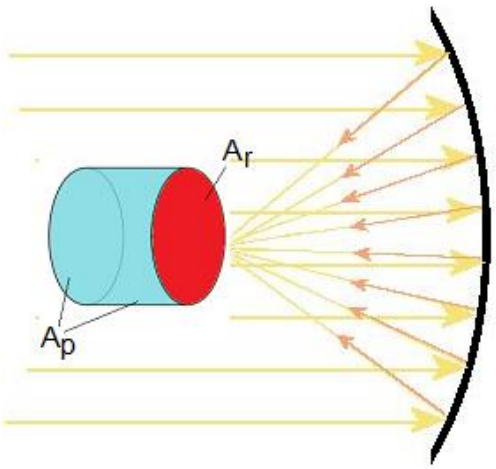

Fig. 8. Hot and Peripheral Surface Area of the Receiver

The heat losses due to wind flow (convection) can be calculated by

$$Q_{conv} = hA_t\Delta T_{conv} \tag{9}$$

where h is the convection heat transfer coefficient (w/m^{2}K), A_t is the total area of the receiver (m^2) given by

$$A_t = A_r + A_p \tag{10}$$

$$h = 10.45 - v + 10\sqrt{v}, \tag{11}$$

and ΔT_{conv} is the difference between the average temperature of the water at the inlet and outlet and the ambient temperature (K), and v is wind speed (m/sec) [29]. Equation (11) is valid for wind speeds up to 20 m/sec [30].

The calculation of heat loss through the receiver's material (conduction) is more complex. It can be driven from

$$Q_{cond} = kA_t\frac{\Delta T}{t} = mc(\Delta T)' \tag{12}$$

where k is the thermal conductivity of stainless steel (W/(m K)), ΔT is the temperature difference between the receiver's and ambient temperature (K), t is the thickness of the receiver (m), m is the mass of the receiver (kg), c is the specific heat capacity of stainless steel 316 sheet, which is 500 J/kg°C, and $(\Delta T)'$ is the receiver's temperature change over a specific time (K/sec).

The receiver's temperature is assumed to be the average water temperature at the inlet and outlet. The Q_{cond} should be calculated under constant sun radiation. Since k, A_t, and t are constant, for any specific temperature difference, Q_{cond} can easily be estimated from the first part of equation 12 [30].

Also, the concentration ratio of the PD (C_{pd}) can be calculated from

$$C_{pd} = \frac{A_a}{A_r} \tag{13}$$

Finally, for exergy evaluation, input exergy, output exergy, and exergy efficiency should be calculated using

$$Ex_{in} = I_{sun}A_a\left(1 - \frac{4}{3}\frac{T_{amb}}{T_{sun}} + \frac{1}{3}\left(\frac{T_{amb}}{T_{sun}}\right)^4\right) \tag{14}$$

$$Ex_{out} = I_{sun}A_a\left(1 - \frac{T_{amb}}{T_{rec\_r}}\right) \tag{15}$$

$$\eta_{ex} = \frac{Ex_{in}}{Ex_{out}} \tag{16}$$

where Ex_{in} is input exergy (watts), Ex_{out} is output exergy (watts), T_{sun} is the temperature of the sun's surface, which is 5778 K [28], and η_{ex} is the exergy efficiency of the PD [29].

3. Results

In this section, the PD concentrator's performance evaluation is presented. First, data of the receiver's maximum surface temperature at the focal point at various sun radiation intensities are measured via Testo 881. Secondly, multiple parameters in Eqs. (4) to (16) are reported at a constant flow rate of water, 0.95 lit/min. Based on these results, further discussion is held to understand how to enhance the performance of the concentrator.

3.1. Receiver's Maximum Temperature

This test was performed on a sunny day on September 13, 2016, in Tehran, Iran, at the Sharif University of Technology. Table 2 shows the results obtained at different hours and radiation levels. Figure 9 shows the maximum temperature on the receiver's hot surface versus the input radiation intensity, which displays a linear dependence. In these measurements, water circulation is stopped.

3.2. Parabolic Dish Evaluation

According to section 2.4., some parameters should be measured to evaluate the PD's efficiency. For this purpose, water is pumped into the receiver. The test was done on October 1, 2016. The measured parameters are reported in table 3, where the concentration ratio (C_{pd}) of the PD in Eq. (13) is equal to 98.

Table 2. The Receiver's Maximum Temperature vs. Incident Radiation Intensity

Time	T_{rec_r}-max (℃)	I_{sun} (W/m^2)	v (m/s)	T_{amb} (℃)
10:30:00	260	762	1.2	26.4
10:35:00	263	782	1.4	26.8
10:40:10	300	794	1.5	26.4
11:12:00	340	866	1.4	26.5
11:20:16	374	904	1.8	28.6
11:27:20	385	922	1	27.7
11:35:23	419	937	1.2	29.3
11:45:05	440	962	1	29
11:56:24	425	986	0.8	29.2
12:05:00	430	995	0	29.7
12:14:00	464	1009	0.9	31.6
12:28:00	473	1035	1.3	29.7
12:32:00	486	1036	1.1	28.3
12:41:00	540	1039	1.6	30.8
12:46:00	533	1056	1	29
12:51:00	520	1030	0	30.9
13:21:00	517	1032	1.9	30.3
13:28:00	509	1025	0.8	29.9
13:33:50	510	1012	0	29.2
13:59:23	491	998	3	31.3

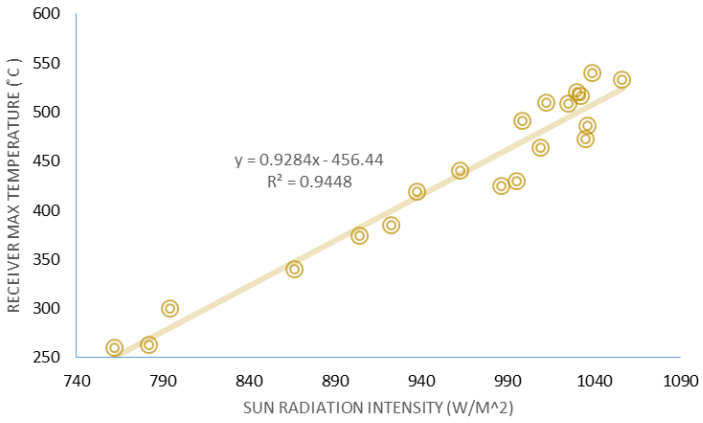

Fig. 9. The Receiver's Maximum Temperature vs. Incident Radiation Intensity

Table 3. Measured Parameters With Water Circulation

Time	I_{sun} (W/m^2)	T_{rec_r} (℃)	Water Inlet Temperature (℃)	Water Outlet Temperature (℃)	v (m/s)	T_{amb} (℃)
10:44:00	849	320	23	44	2.4	24.8
10:48:00	864	333	23	45	3.3	23.4
11:02:00	941	380	32	55	3.1	24.8
11:06:00	951	429	32	53	1.5	24.1
11:09:00	954	432	28	52	0	25.4
11:17:00	975	420	28	49	3.2	24.4
11:30:00	990	442	25	47	1.9	25.5
11:40:00	1008	456	27	51	1.9	25.4
11:55:00	1076	520	28	53	0	26.5
12:00:00	1082	514	27	52	1.9	24.4

Table 4. Energy Results

Time	Q_a (W)	Q_w (W)	h (W/m2K)	Q_{conv} (W)	Q_{rad_r} (W)	Q_{rad_p} (W)	Q_{cond} (W)	Q_{rec} (W)	η_{en}
10:44:00	2554.1	1391.7	23.54	77.2	10.3	0.4	0.6	1480.2	58%
10:48:00	2599.2	1457.9	25.32	101.2	11.3	0.5	0.8	1571.7	60%
11:02:00	2830.9	1524.2	24.96	175.9	15.5	1.0	1.4	1718	61%
11:06:00	2861.0	1391.7	21.20	147	21	0.9	1.4	1562	55%
11:09:00	2870.0	1590.5	10.45	57.5	21.3	0.7	1.1	1671.1	58%
11:17:00	2933.2	1391.7	25.14	133.6	19.9	0.7	1.0	1546.9	53%
11:30:00	2978.3	1457.9	22.33	88.4	22.6	0.5	0.8	1570.2	53%
11:40:00	3032.5	1590.5	22.33	114.5	24.5	0.7	1.0	1731.2	57%
11:55:00	3237.0	1656.8	10.45	55.2	34.5	0.7	1.0	1748.2	54%
12:00:00	3255.1	1656.8	22.33	127.1	33.5	0.8	1.1	1819.3	56%

Table 5. Exergy Results

Time	I_{sun} (W/m^2)	T_{amb} (℃)	T_{rec_r} (℃)	Ex_{in} (W)	Ex_{out} (W)	η_{ex}
10:44:00	849	24.8	320	2427.95	1297.6	53%
10:48:00	864	23.4	333	2471.70	1355.2	55%
11:02:00	941	24.8	380	2691.05	1571.5	58%
11:06:00	951	24.1	429	2720.12	1684.1	62%
11:09:00	954	25.4	432	2727.82	1689.3	62%
11:17:00	975	24.4	420	2788.56	1708.8	61%
11:30:00	990	25.5	442	2830.68	1770.6	63%
11:40:00	1008	25.4	456	2882.22	1828.0	63%
11:55:00	1076	26.5	520	3075.82	2055.9	67%
12:00:00	1082	24.4	514	3094.58	2066.7	67%

Using the parameters in Table 3 the values of incident radiation heat, water absorbed heat, heat losses, and PD energy efficiency are calculated based on Eqs. (4) to (12). The results are shown in Table 4. Since the receiver's surface color is matte black, the radiation heat losses in Eqs. (7) and (8) are calculated by the receiver's surface diffusion coefficient equal to $\epsilon = 0.05$. It should be noted that the center of the concentrator in Fig.3-d is unmirrored, which is subtracted from the energy input.

The analysis of Table 4 indicates that a) the average PD energy efficiency is approximately 57%, b) convection is the most significant heat loss, and c) peripheral surface radiation heat loss Q_{rad_p} and conduction heat loss Q_{cond} are extremely small in comparison to other heat losses.

Finally, Table 5 shows the exergy analysis of the PD concentrator. It shows that as the receiver's hot side temperature rises, the exergy efficiency increases, too.

4. Discussion

According to the energy analysis results presented in Table 4, the incident total heat to the receiver Q_{rec} is always more than 1kW. Due to its energy and exergy efficiencies, the designed PD can be used for regular heating applications, such as cooking, drying, and water heating. However, they may not be applicable for industrial or power generation purposes, and a larger aperture diameter with a more efficient concentrator is required. In order to improve efficiency, some changes should be applied to the components and fabrication process of the PD.

As seen in the upper left part of Fig.3-d, some discontinuities in the mirrors' images existed, which show that the attached mirrors did not follow the PD's curve. Also, in Fig.6, it is apparent that some reflected sunbeams are scattered in the outer area of the receiver's hot surface. The reasons for this scattering, which leads to lower efficiency, are as follows.

4.1. Mirrors' Edges

As mentioned in section 2.1.1., 2 mm glass/silver mirrors with a width of 5 cm and a length of one meter (available on the market at an affordable price) are used as mirrors. The mirrors' edges are not chamfered or well-cut and have approximately a 2 mm deviation, which makes the edges not engage perfectly in reflection. Thus, the radiated sunbeams on the edges are scattered and not reflected on the receiver. The total edges of the adhered mirrors on the PD are 76 m, which equals 0.304 m^2 of the aperture surface. This fault results in a 10% loss of energy efficiency.

This fabrication error can be avoided by using 8cmx8cm mirrors with well-cut or chamfered edges on the PD surface [26]. However, this type of mirror was expensive and not available on the market at the time of fabrication and had to be imported into Iran.

4.2. Mirrors' Flexibility

Mirrors' flexibility helps them to follow the parabolic curve properly. Glass has a Young modulus of nearly 50 GPa and is flexible enough at low thicknesses. Nevertheless, since the mirrors were mounted vertically, 2 mm is not enough flexibility to conform to the parabolic curve. There are some solutions to this problem:

1. The same mirrors can be patterned radially to eliminate the twist due to the parabolic shape.
2. Using mirrors with less thickness would improve the flexibility of the mirror. However, these mirrors were very expensive and were not available on the market at the time of fabrication, so they had to be imported into Iran.
3. Using square mirrors with a small area would follow the parabolic curve better.

5. Conclusions

This study attempts to develop a low-cost fabrication process for solar PD concentrators incorporated with one-meter-long glass/silver mirrors. A solar PD is designed, fabricated, and evaluated with a 2 m aperture diameter at the Sharif University of Technology. A cylindrical stainless steel 316 receiver colored with high-temperature resistant matte black is utilized with water as the heating fluid to evaluate the PD. The results show that the concentration ratio is 98. The highest temperature observed on the receiver's hot surface is 540 ℃. The average energy efficiency is 57%, and the maximum exergy efficiency is 67%. The maximum heat absorbed by the pumped water is 1656.8 watts at midday with a radiation intensity of 1082 W/m^2.

For regular thermal applications, this type of fabrication is suitable. However, several deficiencies are detected, and some solutions are proposed. PD's performance is affected by the edges and the flexibility of the mirrors. Small square mirrors instead of the current one-meter mirror would reduce scattering and increase PD efficiency. The square shape mirror helps follow the parabolic curve better, eliminates scattering on mirrors' edges, and minimizes the space between mirrors. For further research, it is recommended to investigate the effects of mirrors' block sticking patterns (i.e. radially, vertically, or horizontally) and the mirror's thickness on the PD's efficiency.

References

[1] Y. Zhang, M. Sivakumar, S. Yang, K. Enever, and M. Ramezanianpour, "Application of solar energy in water treatment processes: A review," Desalination, vol. 428, pp. 116–145, Feb. 2018, doi: 10.1016/J.DESAL.2017.11.020.

[2] M. M. Aboelmaaref et al., "Hybrid solar desalination systems driven by parabolic trough and parabolic dish CSP technologies: Technology categorization, thermodynamic performance and economical assessment," Energy Convers Manag, vol. 220, p. 113103, Sep. 2020, doi: 10.1016/J.ENCONMAN.2020.113103.

[3] N. Abas, A. Kalair, and N. Khan, "Review of fossil fuels and future energy technologies," Futures, vol. 69, pp. 31–49, May 2015, doi: 10.1016/J.FUTURES.2015.03.003.

[4] A. Jamar, Z. A. A. Majid, W. H. Azmi, M. Norhafana, and A. A. Razak, "A review of

water heating system for solar energy applications," International Communications in Heat and Mass Transfer, vol. 76, pp. 178–187, Aug. 2016, doi: 10.1016/J.ICHEATMASSTRANSFER.2016.05.028.

[5] J. Gong, C. Li, and M. R. Wasielewski, "Advances in solar energy conversion," Chem Soc Rev, vol. 48, no. 7, pp. 1862–1864, Apr. 2019, doi: 10.1039/C9CS90020A.

[6] T. Ramachandran, A.-H. I. Mourad, and F. Hamed, "A Review on Solar Energy Utilization and Projects: Development in and around the UAE," Energies 2022, Vol. 15, Page 3754, vol. 15, no. 10, p. 3754, May 2022, doi: 10.3390/EN15103754.

[7] N. A. Handayani and D. Ariyanti, "Potency of solar energy applications in Indonesia. Int," Journal of Renewable Energy Development, vol. 1, no. 2, p. 2012, 2012.

[8] N. Kannan and D. Vakeesan, "Solar energy for future world: - A review," Renewable and Sustainable Energy Reviews, vol. 62, pp. 1092–1105, Sep. 2016, doi: 10.1016/J.RSER.2016.05.022.

[9] S. A. Kalogirou, "solar thermal collectors and applications progress in energy and combustion science, edition: London," Washington DC, 2004.

[10] S. Kalogirou, "Recent patents in solar energy collectors and applications," Recent Patents on Engineering, vol. 1, no. 1, pp. 23–33, 2007.

[11] S. Mekhilef, R. Saidur, and A. Safari, "A review on solar energy use in industries," Renewable and Sustainable Energy Reviews, vol. 15, no. 4, pp. 1777–1790, May 2011, doi: 10.1016/J.RSER.2010.12.018.

[12] S. K. Natarajan et al., "Experimental analysis of a two-axis tracking system for solar parabolic dish collector," Int J Energy Res, vol. 43, no. 2, pp. 1012–1018, Feb. 2019, doi: 10.1002/ER.4300.

[13] A. Jamar, Z. A. A. Majid, W. H. Azmi, M. Norhafana, and A. A. Razak, "A review of water heating system for solar energy applications," International Communications in Heat and Mass Transfer, vol. 76, pp. 178–187, Aug. 2016, doi: 10.1016/J.ICHEATMASSTRANSFER.2016.05.028.

[14] V. Siva Reddy, S. C. Kaushik, K. R. Ranjan, and S. K. Tyagi, "State-of-the-art of solar thermal power plants—A review," Renewable and Sustainable Energy Reviews, vol. 27, pp. 258–273, Nov. 2013, doi: 10.1016/J.RSER.2013.06.037.

[15] J. Yan, Y. duo Peng, and Z. ran Cheng, "Mirror rearrangement optimization for uniform flux distribution on the cavity receiver of solar parabolic dish concentrator system," Int J Energy Res, vol. 42, no. 11, pp. 3588–3614, Sep. 2018, doi: 10.1002/ER.4104.

[16] H. Hijazi, O. Mokhiamar, and O. Elsamni, "Mechanical design of a low cost parabolic solar dish concentrator," Alexandria Engineering Journal, vol. 55, no. 1, pp. 1–11, Mar. 2016, doi: 10.1016/J.AEJ.2016.01.028.

[17] R. Affandi, C. Gan, and M. R. Ab Ghani, "Development of Design Parameters for the Concentrator of Parabolic Dish (PD) Based Concentrating Solar Power (CSP) under Malaysia Environment," The Journal of Applied Science and Agriculture, vol. 9, pp. 42–48, Jan. 2014.

[18] L. Li and S. Dubowsky, "A new design approach for solar concentrating parabolic dish based on optimized flexible petals," Mech Mach Theory, vol. 46, no. 10, pp. 1536–1548, Oct. 2011, doi: 10.1016/J.MECHMACHTHEORY.2011.04.012.

[19] S. Aljabair, L. J. Habeeb, and A. M. Ali, "EXPERIMENTAL ANALYSIS OF PARABOLIC SOLAR DISH WITH RADIATOR HEAT EXCHANGER RECEIVER," Journal of Engineering Science and Technology, vol. 15, no. 1, pp. 437–454, 2020.

[20] S. M. M. Ahmed, M. R. Al-Amin, S. Ahammed, F. Ahmed, A. M. Saleque, and M. Abdur Rahman, "Design, construction and testing of parabolic solar cooker for rural households and refugee camp," Solar Energy, vol. 205, pp. 230–240, Jul. 2020, doi: 10.1016/J.SOLENER.2020.05.007.

[21] V. P. Stefanovic, S. R. Pavlovic, E. Bellos, and C. Tzivanidis, "A detailed parametric analysis of a solar dish collector," Sus-

tainable Energy Technologies and Assessments, vol. 25, pp. 99–110, Feb. 2018, doi: 10.1016/J.SETA.2017.12.005.

[22] Y. Rafeeu and M. Z. A. Ab Kadir, "Thermal performance of parabolic concentrators under Malaysian environment: A case study," Renewable and Sustainable Energy Reviews, vol. 16, no. 6, pp. 3826–3835, Aug. 2012, doi: 10.1016/J.RSER.2012.03.041.

[23] V. M. Avargani, A. Rahimi, and T. Tavakoli, "Exergetic Optimization and Optimum Operation of a Solar Dish Collector with a Cylindrical Receiver," Journal of Energy Engineering, vol. 142, no. 4, p. 04015049, Dec. 2015, doi: 10.1061/(ASCE)EY.1943-7897.0000322.

[24] P. Savangvong, B. Silpsakoolsook, and S. Kwankoameng, "Design and fabrication of a solar-dish concentrator with 2-axis solar tracking system," IOP Conf Ser Mater Sci Eng, vol. 1137, no. 1, p. 012008, May 2021, doi: 10.1088/1757-899X/1137/1/012008.

[25] S. K. Sahu, K. Arjun Singh, and S. K. Natarajan, "Design and development of a low-cost solar parabolic dish concentrator system with manual dual-axis tracking," Int J Energy Res, vol. 45, no. 4, pp. 6446–6456, Mar. 2021, doi: 10.1002/ER.6164.

[26] E. Gholamalizadeh and J. D. Chung, "Exergy Analysis of a Pilot Parabolic Solar Dish-Stirling System," Entropy, vol. 19, no. 10, 2017, doi: 10.3390/e19100509.

[27] P. R. Fraser, Stirling dish system performance prediction model. 2008.

[28] S. A. Kalogirou, Solar energy engineering: processes and systems. Academic Press, 2013.

[29] R. Petela, "Exergy of Heat Radiation," J Heat Transfer, vol. 86, no. 2, pp. 187–192, May 1964, doi: 10.1115/1.3687092.

[30] J. P. Holman, "Heat transfer." McGraw Hill Higher Education, 2010.